Food Hydrocolloids 25 (2011) 879–886

Contents lists available at ScienceDirect

Food Hydrocolloids

journal homepage: www.elsevier.com/locate/foodhyd

Characterization of quinoa protein–chitosan blend edible films

Lilian E. Abugoch*, Cristián Tapia*, Maria C. Villamán, Mehrdad Yazdani-Pedram, Mario Díaz-Dosque

Departamento de Ciencia de los Alimentos y Tecnología Química, Facultad de Ciencias Químicas y Farmacéuticas, Universidad de Chile, Vicuña Mackenna 20, Santiago, Chile

Keywords:
Quinoa protein
Chitosan
Edible films
Structural properties
Mechanical barrier properties

A B S T R A C T

Quinoa protein/chitosan films were obtained by solution casting of blends of quinoa protein extract (PE) and chitosan (CH). Films from a PE/CH blend were characterized by FTIR, X-ray diffraction, thermal analysis, and SEM. The tensile mechanical, barrier, and sorption properties of the films were also evaluated. The blend of PE with CH yielded mechanically resistant films without the use of a plasticizer. The film had large elongation at break, and its water barrier properties showed that they were more hydrophilic than CH film. The thickness and water-vapor permeability of PE/CH (v/v) 1/1 blend film increased significantly compared to pure CH films. CH films are translucent in appearance and yellowish in blend with PE. By blending anionic PE with cationic CH an interaction between biopolymers was established with different physicochemical properties from those of pure CH. Drying and sorption properties show significant differences between PE/CH blend film and CH film. The structural properties determined by XRD, FTIR and TGA showed a clear interaction between quinoa proteins and CH, forming a new material with enhanced mechanical properties.

1. Introduction

Biopolymers including proteins and chitosan have been the focal point of an expanding number of studies reporting their potential use in new materials, such as edible film. There is sustained development of edible films due to their great potential for food use, since they can be made from a variety of materials to control water and gas diffusion and therefore improve food quality and shelf life (Debeaufort, Quezada-Gallo, & Voilley, 1998; Min & Krochta, 2007; Simelane & Ustunol, 2005; Viroben, Barbot, Mouloungui, & Guéguen, 2000). There are few reports on the characterization and uses of quinoa and even fewer on its proteins (Abugoch, Romero, Tapia, Rivera, & Silva, 2008; Becker & Hanners, 1990; Chauhan, Eskin, & Tkachuk, 1992; Ogungbenle, 2003). Quinoa is described as a seed with high protein content (12–23%) and a highly recommendable amino acid balance for human consumption (Abugoch et al., 2008; Oshodi, Ogungbenle, & Oladimeji, 1999; Ruales, Grijalva, Lopez-Jaramillo, & Nair, 2002). Quinoa protein fractions are 2S albumins and 11S globulins whose structure is stabilized through disulfide bridges (Abugoch et al., 2008; Brinegar & Goundan, 1993; Brinegar, Sine, & Nwokocha, 1996; Fairbanks, Burgener, Robison, Andersen, & Ballon, 1990). Their proteins can give other different properties to the films, extending their use in the food industry. Abugoch et al. (2008) found that quinoa proteins are soluble at both acid and alkaline pH. On the other hand, chitosan has been evaluated for various uses in the food, medical, pharmaceutical, agricultural, and chemical industries because of its nontoxic, biocompatible, mucoadhesive, and biodegradable properties. Chitosan (CH) is the N-deacetylated derivative of chitin, with a degree of deacetylation of not less than 65% (Majeti & Kumar, 2000; Pastor et al., 2004). CH can be dissolved in dilute hydrochloric acid or organic acids such as acetic, lactic, and citric acids, and films are formed simply by solvent evaporation. The cationic nature of chitosan allows ionic interactions with other ionic compounds, leading to new materials. CH is known as a film-forming polymer which can have different mechanical, barrier, and antimicrobial properties (Coma et al., 2002; Myong, Son, Kim, Weller, & Hanna, 2006; Sebti, Chollet, Degraeve, Noel, & Peyrol, 2007). The characteristics of chitosan film, however, vary depending on its source, the solvents used, the methods of film preparation, the drying conditions, and the types and amounts of plasticizers and/or copolymers used (Begin & Van Calsteren, 1999; Cervera et al., 2004; Nunthanid, Puttipipatkhachorn, Yamamoto, & Peck, 2001; Ritthidej, Phaechamud, & Koizumi, 2002). Some studies have reported that films prepared from mixtures seem to improve the physicochemical properties, but additional studies are still needed (Cervera et al., 2004; Debeaufort et al., 1998; Di Pierro et al., 2006; Prodpran, Benjakul, & Artharn, 2007; Schmitt, Sánchez, Desobry-Banon, & Jöel, 1998). Considering that quinoa proteins are soluble at acid pH and CH can be dissolved in organic acids, a complex between quinoa protein and CH would allow making

* Corresponding authors. Tel.: +56 2 9781635/640; fax: +56 2 2227900.
E-mail addresses: labugoch@uchile.cl (L.E. Abugoch), ctapia@uchile.cl (C. Tapia).

0268-005X/$ – see front matter © 2010 Elsevier Ltd. All rights reserved.
doi:10.1016/j.foodhyd.2010.08.008

a film having its own properties potentiated by the mixture of these two biopolymers. There are no reports describing the combination of quinoa protein–chitosan (QP/CH) to make films. Quinoa protein would be able to interact ionically through anionic sulfide groups with the protonated amino groups of chitosan. The combination of both polymers would produce a synergistic effect on the mechanical and adhesive properties of the prepared films because of the excellent elongation and adhesive properties of quinoa proteins, thus avoiding the use of plasticizers. The aim of this work was to prepare edible blend films based on quinoa protein and chitosan with good mechanical and gas barrier properties without the use of auxiliary plasticizers.

2. Materials and methods

2.1. Materials

2.1.1. Preparation of quinoa flour

The organic seeds of quinoa (*Chenopodium quinoa* Willd.) (commercial cultivar) used in this work were grown in the VI Region of Chile and were supplied by "Compañía Procesadora de Semillas de Quinoa Pablo Jara Valdivia, Chile". The defatted quinoa flour (DQF) was obtained according to the method described by Abugoch et al. (2008) and finally stored at 4 °C until use.

2.1.2. Chitosan (CH)

CH from Sigma, USA. The intrinsic viscosity [η] was 1.395 mL/g in 0.3 M acetic acid 0.2 M sodium acetate buffer solution. The viscometric molecular weight of CH was estimated as 408 kDa. The degree of deacetylation was 77.2% (Tapia et al., 2004).

2.1.2.1. Viscosity molecular weight average. Viscosity molecular weight average was determined by using the Mark–Howink constants, $K = 1.81 \times 10^{-3}$ mL/g and $a = 0.93$ reported by Rinaudo, Milas, and Le Dung (1993). For this determination it was necessary to measure the intrinsic viscosity of chitosan solution. Chitosan was dissolved in 0.3 M acetic acid 0.2 M sodium acetate buffer solution according to Rinaudo et al. (1993).

2.1.2.2. Degree of acetylation (DA). Degree of acetylation (DA) was measured by ^{1}H NMR spectroscopy as reported (Lavertu et al., 2003).

2.1.3. Preparation of aqueous protein extract (PE)

DQF was suspended in water (13% w/w) and the pH was adjusted to 9 by adding 2 N NaOH. The suspension was stirred for 30 min at room temperature and then centrifuged at 7000 *g* for 60 min. The PE was prepared and was used immediately every time it was required for the preparation of CH/PE blends. The concentration of the soluble protein fraction of PE was determined by the method described by Bradford (1976), and it was 0.8%. The Bradford (1976) method of protein determination is based on the binding of a dye, Coomassie blue G, to the protein. The pH and turbidity of the centrifuged solutions were also measured.

2.1.4. Preparation of chitosan solutions

Solutions of 1% w/v (pH 3.3) and 2% w/v (pH 2.4) of CH in 1% w/w lactic acid were prepared. The solutions were left overnight and then filtered in a pressure filter (Sartorius model SM16249, Germany) at 586 kPa using a prefilter/absolute filter combination (Sartorius borosilicate microfilter MFS GC50/cellulose nitrate 0.45 μm). The pH of the filtered solutions was measured with a pH meter at 20 °C (pH meter WTW pH330, Germany). The filtered solutions were left overnight at 4 °C to eliminate bubbles.

2.1.5. Viscosity and turbidity

The viscosity of chitosan in a 1% w/w lactic acid filtered solution, of PE, and of blend solution PE/CH 1/1 was measured at 50 rpm using spindle 61 in a rotational viscometer (Brookfield DV-II+Pro, USA). The turbidity of 1% and 2% w/v chitosan in 1% w/w lactic acid filtered solutions was measured at 20 °C in a previously calibrated turbidimeter (Hanna Instruments, model HI 93703, USA).

2.1.6. Water activity (a_w)

Water activity was measured at 25 °C with a thermoconstanter electric hygrometer (Novasina, model TH-200, Switzerland).

2.2. Film formation and drying conditions

2.2.1. Film formation

Blends of PE and CH were prepared by mixing solutions of PE (6.7% w/v) and CH (2% w/v) with different PE/CH v/v ratios (4/1, 1/1, 1/4, 0/1). The pH of the mixtures was adjusted to 3.0 with lactic acid (85% w/v) and stirring was continued for 1 h. The resulting blend solutions were filtered under vacuum. These blends (25 mL) were cast on a horizontal surface in low density polyethylene boxes, measuring 10 cm × 10 cm × 1 cm. The films were dried to constant weight at 50 °C (Sebti et al., 2007). The dried films were removed carefully from the boxes and were conditioned at 22 °C and 60% relative humidity for 3 days before testing.

2.2.2. Determination of the drying curves

To determine the experimental drying curves, the film-forming solutions were left in an oven at a constant temperature of 50 °C. Moisture content at each time interval was calculated from the weight loss data and the dry solid weight of the sample when no further weight loss could be measured. Initial moisture content was determined according to AOAC (1996). The evaporation rate was calculated from Eq. (1).

$$N = \frac{Ls}{A}\left(-\frac{\partial x}{\partial t}\right) \quad (1)$$

where: N = evaporation rate (kg/s.m^2); Ls = dry solid mass (kg dry solid), A = dry area (m^2), ∂x = moisture loss, and ∂t = time (s).

The drying constants, product constant and effective moisture diffusivity were determined from the drying curves (Eq. (2), McCabe, Smith, & Harriot, 1985),

$$\frac{X - X_e}{X_o - X_e} = \frac{8}{\pi^2}\exp\left(-\frac{\pi D_{ef} t}{L^2}\right) \quad (2)$$

where: X = moisture content, X_e = equilibrium moisture content, X_o = initial moisture content (all in kg water/kg dry solid), D_{ef} = effective diffusivity (m^2/s), t = time (s), and L = thickness (m).

D_{ef} was calculated from the slope of the ln $((X - X_e)/(X_o - X_e))$ versus time curve.

2.3. Characterization of the films

2.3.1. Thickness

Film thickness (mm) was determined on four film samples per PE/CH ratio, averaging the measurements at eight points for each film using a digital micrometer (E5010109, VETO & Co.). Similarly, the thickness of the films used for determining water-vapor permeability, elongation, and tensile strength was also measured.

2.3.2. Water activity (a_w)

Water activity was measured according to point 2.1.6.

2.3.3. Mechanical properties of the films

The tensile mechanical properties were determined on a universal tensile testing machine (LLOYD model LR5K, England) provided with a 5 kN load cell and controlled by the DAPMAT VER 3.0 software. Tensile strength (TS) and percent elongation at break (%E) were determined using the Official Chilean Standard method (NCh1151, 1999), equivalent to the ISO R1184-1970 standard method. Four film specimens per PE/CH ratio were cut into 10 mm × 50 mm strips and were tested using a double clamp with a separation of 30 mm at a test speed of 20 mm/min. The curve load versus extension was recorded until the elongation at break was reached. The TS was expressed in MPa and was calculated by dividing the maximum load (N) by the cross-sectional area (m^2). Maximum elongation at break or percent elongation at break (%E) was determined by dividing the extension at the moment of breakage by the initial gauge length of the samples and multiplying by 100. TS and %E values reported are the average of at least four measurements performed for each type of film.

2.3.4. Sorption studies

Saturated solutions of lithium chloride, potassium acetate, magnesium chloride, potassium carbonate, magnesium nitrate, sodium bromide, sodium chloride and potassium chloride were used in desiccators to obtain different relative humidity combinations having a_w values of 0.11, 0.23, 0.33, 0.43, 0.58, 0.76 and 0.85, respectively. All chemicals were of analytical grade from Merck, Darmstadt, Germany. The initial moisture content of the blend films was measured in duplicate on a dry basis (db in %) by drying them to constant weight in a hot air oven at 100 ± 2 °C (AOAC, 1996). Prior to keeping the films, they were conditioned to 53% RH at 23 ± 1 °C. The sorption experiments were carried out by keeping films of 1.5 cm × 1.5 cm in desiccators (~530 mg). The weight of the moisture equilibrated samples was determined in the steady state reached after around 20 days.

2.3.4.1. Sorption models. The Guggenheim–Anderson–de Boer (GAB) model was used to obtain the sorption behavior of the biopolymer blend films and to represent the experimental sorption data according to Eq. (3)

$$X = \frac{X_m C K a_w}{(1 - K a_w)(1 - K a_w + C K a_w)} \quad (3)$$

where: X = moisture content (kg water/kg dry solid), X_m = monolayer value (kg water/kg dry solid), and C (−) and K (−) are constants related to the heat of sorption.

A macro using the GAB equation was designed using Excel software. Linear and nonlinear least-squares regression analyses were used to estimate C, K, and X_m. The ability of the GAB model to fit experimental data was evaluated.

2.3.5. Water-vapor permeability (WVP)

The WVP measurements were carried out according to the Official Chilean Standard method (NCh2098, 2000), equivalent to the ASTM D1653-93 and DIN 52615 standard methods, using the wet cup method and testing six films of each sample. The cup was filled with distilled water to a height of 6 mm from the top edge. The film was sealed to the cup with silica gel. The cup was placed in a room at 22 ± 0.6 °C and 58 ± 2% relative humidity. The weight of the cup was measured daily for 21 days. The WVP was estimated from Eq. (4)

$$WVP = \frac{\Delta m}{t A \Delta P} \varepsilon \quad (4)$$

where: WVP = water-vapor permeability in g m^{-2} h^{-1} Pa^{-1} mm; Δm = mass change over time in g; t = time in h; A = film area in m^2, ΔP = partial vapor pressure difference of the atmosphere with silica gel and pure water (2642 Pa at 22 °C), and ε = thickness in mm.

2.3.6. Film microstructure

The microstructure characterization of the selected films was determined by scanning electron microscopy (SEM) on a Jeol Scanning Electron Microscope (Jeol, JSC 6400, Akishima, Tokio, Japan). Prior to examination, the films were mounted in a 10-mm diameter cylindrical die using double face adhesive tape and were then gold-sputter-coated for 3 min at 20 kV in an argon atmosphere (PELCO 91000) to render them electrically conductive. The images were registered on black and white photographic film (TMX-120 Kodak TMAX 100).

2.3.7. Fourier transform infrared spectroscopy (FTIR)

FTIR measurements were made on a Bruker model IFS 32 spectrometer. About 2 mg of the samples were ground thoroughly with KBr and pellets were formed under a hydraulic pressure of 1.01×10^7 Pa. The characteristic absorption bands were measured for the PE powder, CH powder and the PE/CH = 1/1 (v/v) film. The spectra were obtained by averaging 20 scans in the spectral range of 4000–700 cm^{-1}.

2.3.8. Thermogravimetric analysis

Thermogravimetric analysis (TGA) was performed on a Mettler Toledo TC15 TA controller over the 30–250 °C temperature range at a heating rate of 10 °C/min. The sample weights examined were between 5 and 10 mg. Nitrogen gas flowed over the open crucibles containing the sample as the analysis was performed. The percentage weight loss during the heating cycle was estimated using the associated software. The thermal analysis was carried out on PE powder, CH powder, and PE/CH = 1/1 (v/v) film.

2.3.9. X-ray diffraction

X-ray diffraction measurements were made on a Siemens D-5000 powder X-ray diffractometer with CuKα radiation (λ 1.54 Å), and a 0.02° step and 2 theta range of 1.7–80° were selected to analyze the crystal structure. The X-ray analyses were carried out on PE powder, CH powder, and PE/CH = 1/1 (v/v) film.

2.4. Statistical analysis

Statgraphics plus 5 was used for all statistical analyses. Analysis of variance (ANOVA) and significance of differences between means of Tukey's multiple range tests at a p level of 0.05 were used to determine significance.

3. Results and discussion

3.1. Thickness

The thickness of the films is shown in Table 1. It ranged from 0.054 to 0.142 mm, indicating that the thickness of the films was

Table 1
Tensile strength, elongation at break and thickness of PE/CH blend films.

PE/CH blend film with different composition	Thickness (mm)	Elongation at break (E) (%)	Tensile strength (MPa)
4/1	nff	nff	nff
1/1	$0.142^a \pm 0.017$	$273.4^a \pm 21.6$	$2.3^a \pm 0.5$
1/4	$0.125^b \pm 0.017$	$117.4^b \pm 7.1$	$8.3^b \pm 0.1$
0/1	$0.054^c \pm 0.003$	$73.6^c \pm 8.2$	$22.2^c \pm 3.9$

Different letter means significant differences ($p < 0.05$); nff: no film formation.

significantly higher ($p < 0.05$) for blend film with higher protein extract (PE) proportion (1/1). Film thickness depended on the film's nature and composition (Table 1). This observation agrees with that of Sebti et al. (2007), who found a possible relationship between film thickness and film-forming polymer content and nature, and also with that of Di Pierro et al. (2006).

3.2. Mechanical properties

The tensile strength (TS) and elongation at break (%E) results for PE/CH blend films are shown in Table 1. The TS values of 1/1 PE/CH blend films (2.3 ± 0.5 MPa) were significantly ($p < 0.05$) lower than those of pure chitosan films (22.2 ± 3.9 MPa) and 1:4 PE/CH blends. Compared to the TS values of other edible films that contain proteins and CH, such as whey proteins/CH (Pereda, Aranguren, & Marcovich, 2008), 1/1 whey protein/CH films had similar TS (2.4 MPa) as PE/CH films (2.3 MPa).

The mean elongations at break (%E) values are presented in Table 2. Compared to films made with other biopolymers (wheat gluten, corn zein protein, and soy protein isolate), CH films had significantly higher %E values (Cunningham, Ogale, Dawson, & Acton, 2000). The results show that the presence of PE in the film increased the extensibility up to four times compared to films made only from CH. Elongation at break values of 1/1 PE/CH film was higher than that of CH film, 273.4% and 73.6%, respectively. During CH film formation, hydrogen bonding takes place. When quinoa protein is blended with CH, different molecular interactions between these macromolecules are established, such as ionic and hydrophobic interactions. Also proteins can interact through disulfide bonds when they are denatured (Mauri & Añón, 2008). The 1/1 PE/CH film was chosen initially to continue the characterization, prioritizing its remarkable %E and TS values.

3.3. Physicochemical properties

Some physicochemical characteristics of film-forming biopolymer solutions and the resulting biopolymer films are shown in Table 2. There are differences in viscosity and turbidity between the different film-forming solutions. Table 2 shows that the PE/CH blend solution has higher viscosity than the PE solution and lower viscosity than the CH solution, indicating that interactions occurs between these biopolymers when PE and CH solutions are blended at pH 3. On the other hand, PE solution has higher turbidity than the PE/CH blend film, while CH solution presents less turbidity. It was also found that chitosan films were transparent, while the PE/CH (1/1 v/v) blend film had a yellowish color. We also found differences between a_w values of the films, where the blend film had a lower a_w value than the CH film, indicating that free water in the blend film is less than in the CH film. The possible explanation is that probably the soluble quinoa proteins are interacting ionically with CH and water molecules, contributing to decrease the value of a_w.

Table 2
Physicochemical properties of film-forming biopolymer solutions and films.

Solution or film	Viscosity mPa s	Turbidity (FTU)	a_w	WVP (g mm h^{-1} m^{-2} Pa^{-1})
PE (0.8%)	10 ± 0^a	691.3 ± 157.2^a	–	–
PE/CH (1/1)	50 ± 0^b	375.3 ± 39.6^b	0.360 ± 0.03^a	$9.4 \cdot 10^{-4} \pm 8.5 \cdot 10^{-5a}$
CH (1%)	368^c	47.7 ± 0^c	0.605 ± 0.04^b	$3.8 \cdot 10^{-4} \pm 2.3 \cdot 10^{-5b}$

Different letter means significant differences within the same column ($p < 0.05$).

3.4. Drying kinetics of biopolymer films

The drying curves of the PE/CH 1/1 blend film and CH film are presented in Fig. 1, where the graphs show different behavior, where the initial water content was 30.3 ± 0.1 kg water/kg dry solid for the blend and 35.1 ± 0 kg water/kg dry solid for CH. The drying time needed to reach the critical moisture content was also different, 4.7 h for blend film and 2.3 h for CH film. The equilibrium time for PE/CH blend film (8 h) was higher than that for CH film (5 h). The evaporation rate was similar ($p > 0.05$) for both PE/CH blend film and CH film. It is seen that under the same drying conditions the effect of the nature of the film on the drying curve is different. Calculated effective diffusion coefficients were significantly different ($p < 0.05$), $4.1 \times 10^{-9} \pm 6 \times 10^{-10}$ (m^2/s) for the PE/CH blend film and $9.6 \times 10^{-9} \pm 4 \times 10^{-10}$ (m^2/s) for the CH film.

3.5. Sorption isotherms

The moisture sorption isotherm allows the characterization of the water absorption property of the film, and that knowledge of the sorption isotherm is also important for predicting stability and quality changes during the packaging of food products. Experimental data for moisture adsorption at 25 °C for PE/CH blend and CH films (Fig. 2) showed typical sigmoid-shaped curves for both. At high a_w the moisture content of the PE/CH film increases more than that of the CH film, showing differences ($p < 0.05$) between those films at high water activity values (over 0.6). In a higher water content range the PE/CH blend films were more hydrophilic than CH films. This increase was shown to cause swelling as water activity increased (Sebti et al., 2007). Addition or removal of water may cause phase transitions in the macromolecular structure. The GAB molecular model of adsorption was used to fit the water adsorption data of the films. The GAB equation has been claimed to predict the moisture sorption of proteins and chitosan with adequate accuracy (Cho & Rhee, 2002; Despond, Espuche, & Domard, 2001). To apply the GAB model the second-degree polynomial equation was used. Good agreement between experimental and predicted data was found with the GAB model, with a coefficient of determination (r^2) of 0.988 for PE/CH blend film and 0.992 for CH film. The values of the monolayer (X_m), which indicate the amount of water that is strongly adsorbed to specific sites and is considered as the optimum value at which a film is most stable, were 0.23 g/g for PE/CH blend film (db) and 0.20 g/g (db) for CH

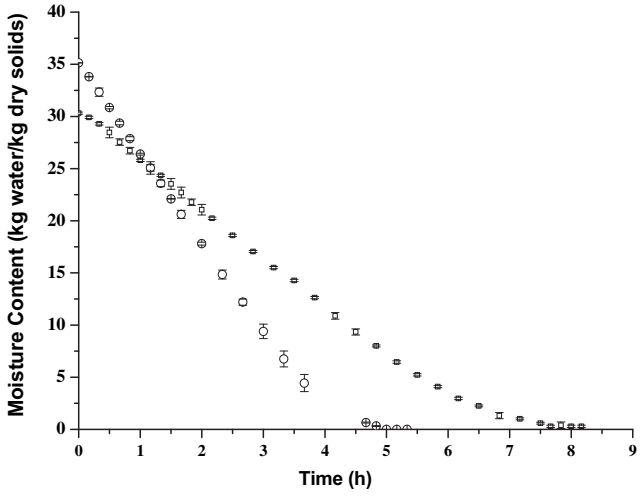

Fig. 1. Experimental drying curves for PE/CH blend film (□) and CH (○) film at 50 °C.

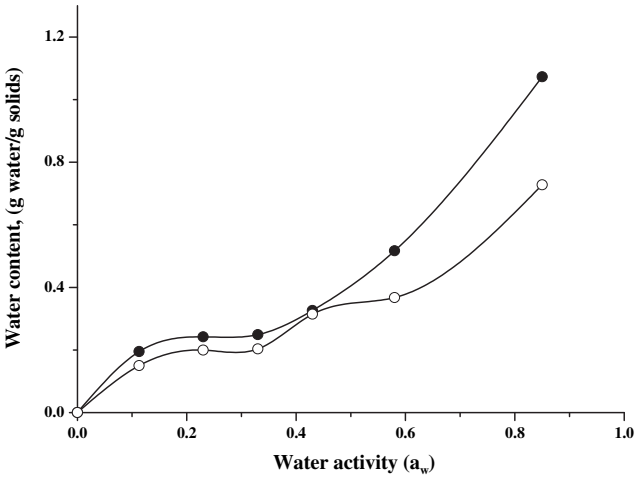

Fig. 2. Sorption isotherms for quinoa proteins-chitosan (PE/CH) blend film (●) and CH (○) film at 25 °C.

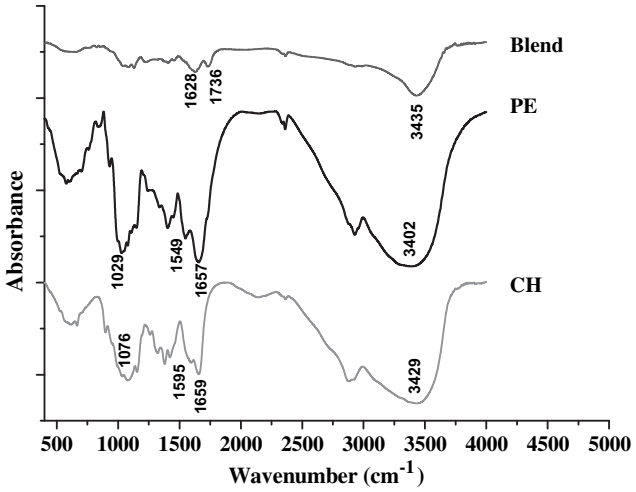

Fig. 4. FTIR spectra of PE, CH, and PE/CH blend film.

film. Small values for the monolayer moisture content were found for the PE/CH blend film and CH film, with the structured water as a monolayer interacting mostly through hydrogen bonds with proteins or CH. Constant C, related to water/substrate interaction energy, was similar for both films (18.9 for PE/CH blend film and 18.7 for CH film), and water molecules were adsorbed with similar energy on the active site. The *k* parameter of the GAB model, which determines the profile at the higher activity range, regulating the upswing after the plateau (Timmermann, 2003), was dependent on the film. The PE/CH blend film had a much higher value (0.932) than the CH film (0.871).

3.6. Water-vapor permeability (WVP)

Table 2 shows the WVP of the films. These values were significantly ($p < 0.05$) lower for CH film than for the PE/CH blend film. The presence of quinoa proteins resulted in increased WVP. This increase was also observed by Di Pierro et al. (2006), who they found that the addition of whey proteins to a CH matrix increased its WVP. Compared to other films that contain CH-corn starch the WVP found was similar to that of PE/CH films (García, Pinotti, & Zaritzky, 2006). The effect found in this research may be related to the hydrophilic character and the thickness of the PE/CH blend films. The influence of film thickness on WVP found in this study has been reported by others (Denavi, Pérez-Mateos, Añón, Montero, Mauri, & Gómez-Guillén, 2009; McHugh, Avena-Bustillos, & Krochta, 1993).

3.7. Changes in crystal structure

The XRD of chitosan powder shows two main diffraction peaks at 2θ 10.1° and 20.1° which agree with previously published results (Ritthidej et al., 2002; Zhang, Wang, Li, Xu, & Zhang, 2009). The XRD of PE showed only one major peak at 2θ 20.1°. There is no information in the literature on XRD of quinoa proteins, but for soy protein isolate a strong characteristic diffraction peak at 2θ 22° has been described (Su, Huang, Yuan, Wanga, & Li, 2010). The diffraction pattern of quinoa protein extract-chitosan blends (Fig. 3) has sharp and well-defined characteristic peaks at 2θ 20–21.5°, 29.7°, 31.2° and 36.1°. The intensity of the diffraction peak of the PE/CH blend film at 2θ 20.1°, compared with chitosan and PE, became flatter and broader, which means that there is good compatibility between both polymers. New diffraction peaks at 2θ 29.7°, 31.2° and 36.1° suggest the existence of intermolecular interactions between quinoa protein (PE) and CH. Since chitosan

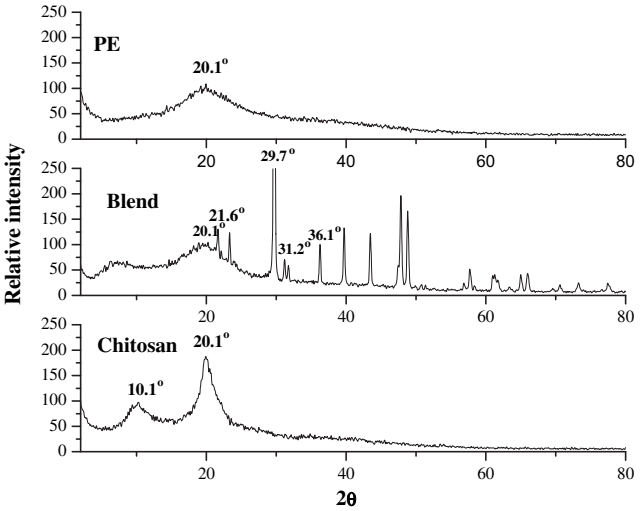

Fig. 3. XRD patterns of PE powder, PE/CH blend film, and CH powder.

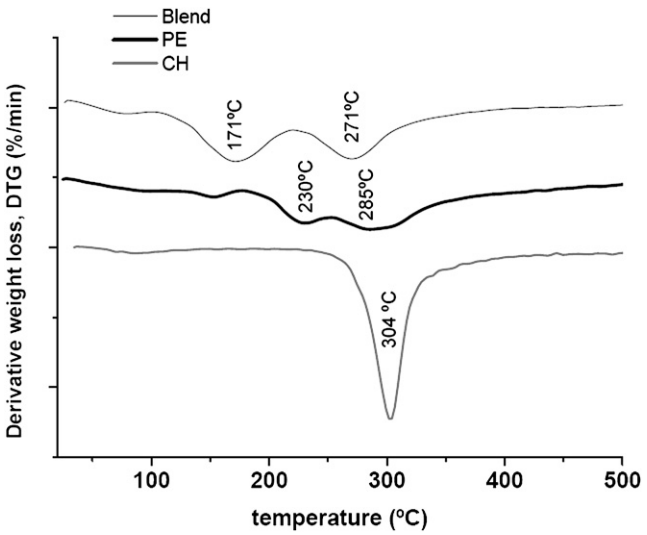

Fig. 5. DTG (%/min) curves of CH, PE, and PE/CH blend film.

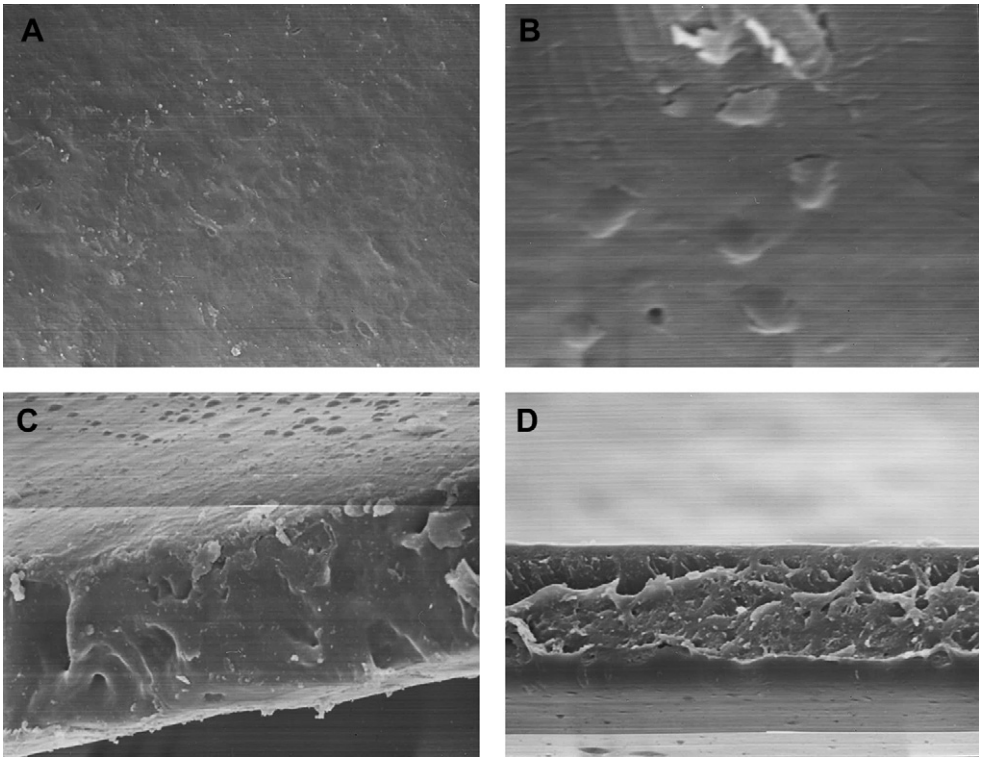

Fig. 6. SEM micrographs of the surface and cross section of 1/1 quinoa protein–chitosan (PE/CH) blend film. A) surface (4500×); B) surface (4500×); C) cross section (700×); D) cross section (700×).

has a rigid, stereo-regular structure containing bulky pyranose rings, the formation of PE/CH can induce a conformational change of the other polyelectrolyte, if the latter has a non-rigid structure (Cerrai, Guerra, & Tricoli, 1996; Park, 1996; Taravel & Domard, 1995).

3.8. Fourier transform infrared spectroscopy (FTIR)

Fig. 4 shows the FTIR spectrum of PE powder, CH powder, and PE/CH blend film. A significant shift of the broad absorption band due to the O–H vibration of PE at 3402 cm^{-1}–3435 cm^{-1} is seen for the PE/CH blend film. The absorption bands seen for PE at 1657 cm^{-1} and 1549 cm^{-1} associated with –NH groups are in agreement with the amide I and amide II bands, respectively. These absorption bands have been reported for soy protein (Su et al., 2010). The absorption bands at 1659 cm^{-1} and 1595 cm^{-1} are assigned to the amide I and amide II bands of CH, respectively. The assignment of these absorption bands are in agreement with those reported for chitosan (Pastor et al., 2004). Also, the blend showed a significant shift of these bands to 1736 cm^{-1} for amide I and 1628 cm^{-1} for amide II, compared with PE and CH. The broad band at approximately 1029 cm^{-1} for PE may be assigned to a contribution of different groups such as out-of-plane C–H bending (from aromatic structures) (Schmidt, Giacomelli, & Soldi, 2005; Su et al., 2010) and PO^{-2} or P–OH stretching from phosphate esters, which are present in significant amounts in soy protein isolate (Schmidt et al., 2005). In the case of CH, the broad absorption band seen at 1076 cm^{-1} is attributed to skeletal vibrations of the pyranose structure of CH (Pastor et al., 2004). These results point out that the main interaction between PE and CH in the blend film would be through the formation of hydrogen bonds, as has been suggested by other authors (Ma & Liu, 2008; Wang, Wang, Dan, Zhang, & Ye, 2006; Zhang et al., 2009).

3.9. TGA analysis

Fig. 5 shows the first derivative weight loss (DTG) curves for CH, PE and PE/CH blend film. The PE/CH blend film had a lower decomposition temperature, with two main weight losses at 171 °C and 271 °C, compared to PE with two main weight losses at 230 °C and 285 °C, and CH with one main weight loss at 304 °C. It has been described that the weight loss due to the decomposition of CH starts at 240 °C and reaches a maximum at 380 °C, with a 41.4% weight loss (Neto et al., 2005), and the main weight loss seen at 304 °C for CH is assigned to CH degradation. Schmidt et al. (2005) have described that the degradation of soy protein isolate films takes place in a single process that begins at 292 °C, reaching the maximum degradation rate at 331 °C. But Su et al. (2010) have reported a lower decomposition temperature (about 110 °C) for soy protein isolate. In this work we observed that the range of decomposition temperature for PE is between 230 and 285 °C. It is clear from the results that the thermal stability of blend film is decreased compared to CH and PE.

3.10. Determination of PE/CH blend film microstructure by SEM

The 1/1 PE/CH blend film was chosen due to its good mechanical and other properties. The scanning electron micrographs of PE/CH (1/1) blend film are shown in Fig. 6. The SEM revealed that the structure of PE/CH blend film was homogeneous and continuous and is comparable with that of edible films from whey proteins (Gupta & Magee, 2007) or oleic acid/CH films (Vargas, Albors, Chiralt, & González-Martínez, 2009). It is clearly seen from the micrographs that both the surface (Fig. 6a and b) and cross section (Fig. 6c and d) of PE/CH blend film is smooth, and a compact structure is also seen (Fig. 6c and d). According to many authors (Pinotti, García, Martino, & Zaritzky, 2007; Vargas et al., 2009), the surface of CH films presents

a smooth, continuous and compact structure. This means that the presence of quinoa protein does not cause discontinuities or porous structures when it is blended with CH.

4. Conclusions

By blending anionic PE with cationic CH, interactions between these biopolymers was established, showing different physicochemical properties compared to CH. The PE/CH blend allowed film formation without the presence of a plasticizer. On the other hand, film prepared from PE/CH (1/1 v/v) solutions had greater thickness than that prepared from CH solution. Moreover, PE/CH blend film showed extremely higher elongation at break compared with that of CH, indicating the internal plasticizing effect of PE in the blend. Drying and sorption properties show a particular behavior in the PE/CH (1/1) blend film, which is more hydrophilic than CH film. Moreover, the structural properties of PE/CH blend film determined by XRD, FTIR and TGA analyses showed good compatibility between both polymers. The main interactions were through hydrogen bonds, and it was also found that the thermal stability of blend film decreases compared to CH and PE. Interactions occur between PE and CH, leading to the formation of a new material with better mechanical and water-vapor permeability properties than CH. Furthermore, the prepared blend films may be used as edible films for packaging purposes in the food industry.

References

Abugoch, L., Romero, N., Tapia, C., Rivera, M., & Silva, J. (2008). Study of some physicochemical and functional properties of quinoa (*Chenopodium Quinoa* Willd.) protein isolates. *Journal of Agricultural and Food Chemistry, 56*(12), 4745–4750.

AOAC. (1996). *Official methods of analysis of AOAC international* (16th ed.). Gaithersburg USA: AOAC International.

Becker, R., & Hanners, G. (1990). Compositional and nutritional evaluation of quinoa whole grain flour and mill fractions. *Lebensmittel-Wissenschaft Und-Technologie, 23*, 441–444.

Begin, R., & Van Calsteren, M. (1999). Antimicrobial films produced from chitosan. *International Journal of Biological Macromolecules, 26*, 63–67.

Bradford, M. M. A. (1976). Rapid and sensitive method for the quantitation of micrograms quantities of protein utilizing the principle of protein-dye binding. *Analytical Biochemistry, 72*, 248–254.

Brinegar, C., & Goundan, S. (1993). Isolation and characterization of chenopodin the 11S seed storage protein of quinoa (*Chenopodium quinoa*). *Journal of Agricultural and Food Chemistry, 41*, 182–185.

Brinegar, C., Sine, B., & Nwokocha, L. (1996). High-cysteine 2S seed storage proteins from quinoa (*Chenopodium quinoa*). *Journal of Agricultural and Food Chemistry, 44*, 1621–1623.

Cerrai, P., Guerra, G., & Tricoli, M. (1996). Polyelectrolyte complexes obtained by radical polymerization in the presence of chitosan. *Macromolecules Chemistry and Physics, 197*, 3567–3579.

Cervera, M., Heinamaki, J., Krogars, K., Jorgensen, A., Karjalainen, M., Colarte, A., et al. (2004). Solid-state and mechanical properties of aqueous chitosan – amylose starch films plasticized with polyols. *AAPS Pharmscitech, 5*, 1–6.

Chauhan, G., Eskin, N., & Tkachuk, R. (1992). Nutrients and antinutrients in quinoa seed. *Cereal Chemistry, 69*, 85–88.

Cho, S., & Rhee, R. (2002). Sorption characteristics of soy protein films and their relation to mechanical properties. *Lebensmittel-Wissenschaft Und-Technologie, 35*, 151–157.

Coma, V., Martial-Gros, A., Garreau, S., Copinet, A., Salin, F., & Deschamps, A. (2002). Edible antimicrobial films based on chitosan matrix. *Journal of Food Science, 67*, 1162–1169.

Cunningham, P., Ogale, A., Dawson, P., & Acton, J. (2000). Tensile properties of soy protein isolate films produced by a thermal compaction technique. *Journal of Food Science, 65*, 668–671.

Debeaufort, F., Quezada-Gallo, J., & Voilley, A. (1998). Edible films and coatings: tomorrows packings: a review. *Critical Reviews in Food Science and Nutrition, 38*, 299–313.

Denavi, G., Pérez-Mateos, M., Añón, M., Montero, P., Mauri, A., & Gómez-Guillén, C. (2009). Structural and functional properties of soy protein isolate and cod gelatin blend films. *Food Hydrocolloids, 23*, 2094–2101.

Despond, S., Espuche, E., & Domard, A. (2001). Water sorption and permeation in chitosan films: relation between gas permeability and relative humidity. *Journal of Polymer Science Part B – Polymer Physics, 39*, 3114–3126.

Di Pierro, P., Chico, B., Villalonga, R., Mariniello, L., Damiao, A., Masi, P., et al. (2006). Chitosan-whey protein edible films produced in the presence of transglutaminase: analysis of their and barrier properties. *Biomacromolecules, 7*, 744–749.

Fairbanks, D., Burgener, K., Robison, L., Andersen, W., & Ballon, E. (1990). Electrophoretic characterization of quinoa seed proteins. *Plant Breeding, 104*, 190–195.

García, A., Pinotti, A., & Zaritzky, N. (2006). Barrier and mechanical properties of biodegradable composite films based on corn starch and chitosan. *Starch/Starke, 58*, 453–463.

Gupta, B., & Magee, M. (2007). Textural properties of whey based edible films. *Electronic Journal of Environmental Agriculture and Food Chemistry, 6*, 2282–2289.

Lavertu, M., Xia, Z., Serreqi, A., Berrada, M., Rodrigues, A., Wang, D., et al. (2003). A validated 1H NMR method for the determination of the degree of deacetylation of chitosan. *Journal Pharmaceutical Biomedical Analyzes, 32*, 1149–/1158.

Ma, J., & Liu, M. (2008). PP non-woven specialties via chemical degradation. *Polymer Material Science Engineering, 24*, 147–150.

McCabe, W., Smith, J., & Harriot, P. (1985). *Drying of solids: unit operations of chemical engineering* (4th ed.). USA: McGraw-Hill. (pp. 717–722).

McHugh, H., Avena-Bustillos, R., & Krochta, J. (1993). Hydrophilic edible films: modified procedure for water vapor permeability and explanation of thickness effects. *Journal of Food Science, 58*(4), 899–903.

Majeti, N., & Kumar, R. (2000). A review of chitin and chitosan applications. *Reactive & Functional Polymers, 46*, 1–27.

Mauri, A., & Añón, M. (2008). Mechanical and physical properties of soy protein films with pH-modified microstructures. *Food Science and Technology International, 14*, 119–125.

Min, S., & Krochta, J. (2007). Ascorbic acid-containing whey protein film coatings for control of oxidation. *Journal of Agricultural and Food Chemistry, 55*, 2964–2969.

Myong, K., Son, J., Kim, S., Weller, C., & Hanna, M. (2006). Properties at chitosan films as a function of pH and solvent type. *Journal of Food Science, 71*, E119–E124.

NCh1151.Of76. (1999). Norma Chilena Oficial: Láminas y películas plásticas – Determinación de las propiedades de tracción (13 pp.).

NCh2098.Of2000. (2000). Norma Chilena Oficial: Películas de recubrimiento orgánico – Determinación de la transmisión de vapor de agua (13 pp.).

Neto, C., Giacometti, J., Jobb, A., Ferreira, F., Fonseca, J., & Pereira, M. (2005). Thermal analysis of chitosan based networks. *Carbohydrate Polymers, 62*, 97–103.

Nunthanid, J., Puttipipatkhachorn, S., Yamamoto, K., & Peck, G. (2001). Physical properties and molecular behavior of chitosan films. *Drug Development and Industrial Pharmacy, 27*, 143–157.

Ogungbenle, H. (2003). Nutritional evaluation and functional properties of quinoa (*Chenopodium quinoa*) flour. *International Journal of Food Sciences and Nutrition, 54*, 153–158.

Oshodi, A., Ogungbenle, H., & Oladimeji, M. (1999). Chemical composition nutritionally valuable minerals and functional properties of benniseed pearl millet and quinoa flours. *International Journal of Food Sciences and Nutrition, 50*, 325–331.

Park, W. (1996). Insoluble polyelectrolyte complex formed from chitosan and α-keratose: conformational change of α-keratose. *Macromolecules Chemistry and Physics, 197*, 2175–2183.

Pastor, A., Agulló, E., Peniche, C., Tapia, C., Argüelles, W., Mayorga Nakamatsu, J. (2004). Quitina y quitosano: obtención carcaterización y aplicaciones. CYTED IV.14 Fondo Editorial PUCP.

Pereda, M., Aranguren, M., & Marcovich, N. (2008). Water vapor absorption and permeability of films based on chitosan and sodium caseinate. *Journal of Applied Polymer Science, 111*(6), 2777–2784.

Pinotti, A., García, M., Martino, M., & Zaritzky, N. (2007). Study on microstructure and physical properties of composite films based on chitosan and methylcellulose. *Food Hydrocolloids, 21*, 66–72.

Prodpran, T., Benjakul, S., & Artharn, A. (2007). Properties and microstructure of protein-based film from round scad (*Decapterus maruadsi*) muscle as affected by palm oil and chitosan incorporation. *International Journal of Biological Macromolecules, 41*, 605–614.

Rinaudo, M., Milas, P., & Le Dung, P. (1993). Characterization of chitosan. Influence of ionic strength and degree of acetylation on chain expansion. *International Journal of Biological Macromolecules, 15*, 281–285.

Ritthidej, G., Phaechamud, T., & Koizumi, T. (2002). Moist heat treatment on physicochemical change of chitosan salt films. *International Journal of Pharmaceutics, 232*, 11–22.

Ruales, J., Grijalva, Y., Lopez-Jaramillo, P., & Nair, B. (2002). The nutritional quality of an infant food from quinoa and its effect on the plasma level of insulin-like growth factor-1 (IGF-1) in undernourished children. *International Journal of Food Sciences and Nutrition, 53*, 143–154.

Schmidt, V., Giacomelli, C., & Soldi, V. (2005). Thermal stability of films formed by soy protein isolate–sodium dodecyl sulfate. *Polymer Degradation and Stability, 87*, 25–31.

Schmitt, C., Sánchez, C., Desobry-Banon, S., & Jöel, H. (1998). Structure and technofunctional properties of protein-polysaccharide complexes: a review. *Critical Reviews in Food Science and Nutrition, 38*, 689–753.

Sebti, I., Chollet, E., Degraeve, P., Noel, C., & Peyrol, E. (2007). Water sensitivity antimicrobial and physicochemical analyses of edible films based on HPMC and/or chitosan. *Journal of Agricultural and Food Chemistry, 55*, 693–699.

Simelane, S., & Ustunol, Z. (2005). Mechanical properties of heat-cured whey protein-based edible films compared with collagen casings under sausage manufacturing conditions. *Journal of Food Science, 70*, E131–E134.

Su, J., Huang, Z., Yuan, X., Wanga, X., & Li, M. (2010). Structure and properties of carboxymethyl cellulose/soy protein isolate blend edible films crosslinked by Maillard reactions. *Carbohydrate Polymers, 79*, 145–153.

Tapia, C., Escobar, Z., Costa, E., Sapag-Hagar, J., Valenzuela, F., Basualto, C., et al. (2004). Comparative studies on polyelectrolyte complexes and mixtures of chitosan–alginate and chitosan–carrageenan as prolonged diltiazem clorhydrate release systems. *European Journal of Pharmaceutics and Biopharmaceutics, 57*(1), 65–75.

Taravel, M., & Domard, A. (1995). Collagen and its interaction with chitosan. II. Influence of the physicochemical characteristics of collagen. *Biomaterials, 16*, 865–871.

Timmermann, E. (2003). Multilayer sorption parameters: BET or GAB values? *Colloids and Surfaces A: Physicochemistry Engineering Aspects, 220*, 235–260.

Vargas, M., Albors, A., Chiralt, A., & González-Martínez, C. (2009). Characterization of chitosan–oleic acid composite films. *Food Hydrocolloids, 23*, 536–547.

Viroben, G., Barbot, J., Mouloungui, Z., & Guéguen, J. (2000). Preparation and characterization of films from pea protein. *Journal of Agricultural and Food Chemistry, 48*, 1064–1069.

Wang, B., Wang, K., Dan, W., Zhang, T., & Ye, Y. (2006). Konjac glucomannan-collagen-chitosan blend films. *Journal of Biomedicine Engineering, 23*, 102–106.

Zhang, B., Wang, D., Li, H., Xu, Y., & Zhang, L. (2009). Preparation and properties of chitosan–soybean trypsin inhibitor blend film with anti-*Aspergillus flavus* activity. *Industrial Crops and Products, 2*(9), 541–548.